

## RESEARCH ARTICLE

# microRNA-31 modulates skeletal patterning in the sea urchin embryo

Nadezda A. Stepicheva and Jia L. Song\*

**ABSTRACT**

MicroRNAs (miRNAs) are small non-coding RNAs that repress the translation and reduce the stability of target mRNAs in animal cells. microRNA-31 (miR-31) is known to play a role in cancer, bone formation and lymphatic development. However, studies to understand the function of miR-31 in embryogenesis have been limited. We examined the regulatory role of miR-31 in early development using the sea urchin as a model. miR-31 is expressed at all stages of development and its knockdown (KD) disrupts the patterning and function of primary mesenchyme cells (PMCs), which form the embryonic skeleton spicules. We identified that miR-31 directly represses *Pmar1*, *Alx1*, *Snail* and *VegfR7* within the PMC gene regulatory network using reporter constructs. Further, blocking the miR-31-mediated repression of *Alx1* and/or *VegfR7* in the developing embryo resulted in defects in PMC patterning and skeletogenesis. The majority of the mislocalized PMCs in miR-31 KD embryos did not express *VegfR10*, indicating that miR-31 regulates *VegfR* gene expression within PMCs. In addition, miR-31 indirectly suppresses *Vegf3* expression in the ectoderm. These results indicate that miR-31 coordinately suppresses genes within the PMCs and in the ectoderm to impact PMC patterning and skeletogenesis. This study identifies the novel function and molecular mechanism of miR-31-mediated regulation in the developing embryo.

**KEY WORDS:** MicroRNA, Primary mesenchyme cell, Cell patterning, Cell migration, Filopodia, *Alx1*, *Pmar1*, *Snail*, *VegfR*, Vegf signaling, *Strongylocentrotus purpuratus*

**INTRODUCTION**

MicroRNAs (miRNAs) are small endogenous RNAs that regulate a myriad of biological processes, including cell fate specification, cell proliferation and cell movement (Bartel, 2009; Huang and He, 2010). As part of the RNA-induced silencing complex, miRNAs bind to the 3'UTR to mediate the translational repression and/or degradation of their target mRNAs in animal cells (Li and Kowdley, 2012; Friedman et al., 2013; Wilczynska and Bushell, 2015). Every miRNA has multiple mRNA targets and a single mRNA can be regulated by multiple miRNAs (Lewis et al., 2005; Lim et al., 2005; Iwama et al., 2007; Wilczynska and Bushell, 2015).

microRNA-31 (miR-31) is highly evolutionarily conserved and has mostly been examined in the context of cancer, as it targets genes that are involved in cell cycle progression, apoptosis, cell-to-cell adhesion and migration (Schmittgen, 2010; Stuelten and Salomon, 2010; Valastyan and Weinberg, 2010; Augoff et al., 2011;

Yamagishi et al., 2012; Körner et al., 2013). miR-31 targets include integrins  $\alpha 2$ ,  $\alpha 5$ ,  $\alpha V$ ,  $\beta 3$ , radixin, RhoA and WAVE3 (Valastyan and Weinberg, 2010; Augoff et al., 2011; Yamagishi et al., 2012). In addition, miR-31 downregulation is required for osteogenic differentiation, as it targets *Osterix* (*Sp7*) and *Satb2*, which are among the main skeletogenic transcription factors (TFs) in vertebrates (Baglio et al., 2013; Deng et al., 2013a,b, 2014a,b).

To date, no animal knockout models are available for miR-31 and limited studies have been conducted to understand the function of miR-31 in the context of embryogenesis (Schuldt, 2005; Dunworth et al., 2014). To identify the function of miR-31 in the developing embryo, we used the purple sea urchin *Strongylocentrotus purpuratus* as a model. We took advantage of the rich knowledge on the gene regulatory network (GRN), signaling pathways and cell fate specification of the *S. purpuratus* embryo. We found that miR-31 is crucial for the patterning and function of the primary mesenchyme cells (PMCs), which produce the skeleton spicules that are used to support swimming and feeding of the larva (Pennington and Strathmann, 1990; Hart and Strathmann, 1994).

PMCs are specified by the canonical Wnt signaling pathway, as  $\beta$ -catenin enters the posterior blastomeres at the 16-cell stage to activate transcription of the transcriptional repressor *Pmar1* (Guss and Ettensohn, 1997; Oliveri et al., 2003). Activated *Pmar1* in turn inhibits the transcriptional repressor *HesC*, resulting in derepression of the major skeletogenic TFs, including *Alx1*, *Ets1* and *Tbr* (Oliveri et al., 2003; Revilla-i-Domingo et al., 2007). The transcriptional activation of these skeletogenic TFs triggers specification of the large micromeres to become PMCs (Khaner and Wilt, 1991; Koga et al., 2010; Sharma and Ettensohn, 2010; Damle and Davidson, 2011; Sharma and Ettensohn, 2011; Lyons et al., 2014; Saunders and McClay, 2014). *Alx1*, which belongs to the evolutionarily conserved *Cart1/Alx3/Alx4* family of Paired-class homeodomain proteins, plays a central role in the skeletogenesis of sea urchins and vertebrates (Ettensohn et al., 2003; Uz et al., 2010; Damle and Davidson, 2011; McGonnell et al., 2011; Dee et al., 2013). *Alx1* regulates the expression of other TFs and effector genes that are directly involved in spicule formation (biomineralization proteins) and genes involved in PMC motility and patterning (*Snail*, *Twist*, *VegfR10*) (Ettensohn et al., 2003; Sharma and Ettensohn, 2011; Rafiq et al., 2012). Knockdown (KD) of *Alx1* in the sea urchin embryo results in decreased numbers of PMCs, delayed ingression of PMCs, failure to complete epithelial-to-mesenchymal transition (EMT) at mesenchyme blastula stage [24 h post fertilization (hpf)] due to the defects in de-adhesion, and a complete lack of skeletal rod formation (Ettensohn et al., 2003; Saunders and McClay, 2014). One of the downstream genes activated by *Alx1* is *Snail*, which encodes an evolutionarily conserved TF that plays a key role in cell migration and EMT in sea urchin and other animals by inhibiting the transcription of cadherin gene and promoting its endocytosis (Bartle et al., 2000; Wu and McClay, 2007; Yuan et al., 2013; Saunders and McClay, 2014).

Department of Biological Sciences, University of Delaware, Newark, DE 19716, USA.

\*Author for correspondence (jsong@udel.edu)

Received 29 June 2015; Accepted 3 September 2015

Following ingressions into the blastocoel, PMCs undergo reproducible patterning that is controlled by both PMC-derived factors and ectodermal positioning cues (Duloquin et al., 2007; Adomako-Ankomah and Ettensohn, 2013; McIntyre et al., 2013). The PMCs migrate along the sides of the blastocoel to form a subequatorial, ventrolateral ring, followed by the bilateral aggregation of PMCs to form the two ventrolateral clusters (VLCs), which are the sites of initial skeletogenic tri-radiate rudiments. The VLCs are formed at the intersections between the border ectoderm (BE) and dorsal-ventral margin (DVM) domains (Duloquin et al., 2007; Adomako-Ankomah and Ettensohn, 2013; McIntyre et al., 2013). The BE is defined as a narrow boundary region between the endoderm and ectoderm and is established by short-range Wnt5 signaling from endodermal cells to the adjacent ectodermal cells (McIntyre et al., 2013). The DVM is a region that separates the dorsal and ventral ectoderm and later becomes the ciliary band (Duboc et al., 2010; Saudemont et al., 2010; Yaguchi et al., 2010). Once the initial VLCs are established, the PMCs undergo another phase of directed migration anteriorly in response to Vegf and Fgf signaling pathways (Duloquin et al., 2007; Adomako-Ankomah and Ettensohn, 2013). Vegf3 is a key ligand expressed in the ectoderm that is crucial for proper PMC patterning. The *S. purpuratus* embryo expresses two Vegf receptors, namely *VegfR7* and *VegfR10*, with *VegfR10* being expressed specifically in the PMCs and thought to be the receptor for Vegf3 (Lapraz et al., 2006; Sodergren et al., 2006; Duloquin et al., 2007; Adomako-Ankomah and Ettensohn, 2013). Unlike *VegfR10*, which has a

unique structure with ten Ig domains, *VegfR7* has the canonical seven Ig domains, making it the most likely ortholog of vertebrate *VegfR* proteins (Lapraz et al., 2006).

In this study, we identified that miR-31 loss of function results in defective PMC patterning, decreased skeletal spicule length, and extra spicule tri-radiates. We present evidence that miR-31 directly suppresses at least three TF (*Pmar1*, *Alx1* and *Snail*) and one effector (*VegfR7*) gene within the PMC GRN using reporter constructs. miR-31 KD also induced aberrant transcriptional expression of *Vegf3*, *VegfR10* and *VegfR7*. The blockage of miR-31 regulation of *Alx1* and/or *VegfR7* in the developing embryo resulted in similar phenotype to that of miR-31 KD embryos, indicating that miR-31 KD phenotypes are in part explained by the lack of miR-31 regulation within PMCs. Overall, this study reveals the molecular mechanism of miR-31-mediated regulation of PMC patterning and function in the developing embryo.

## RESULTS

### miR-31 is ubiquitously expressed throughout development of the sea urchin embryo

Using fluorescent RNA *in situ* hybridization (FISH), we found that miR-31 is expressed throughout early development of the sea urchin embryo and localizes in punctate structures (Fig. 1A). We also observed a reduction of the miR-31 *in situ* signal in embryos microinjected with miR-31 inhibitor, indicating that miR-31 is strongly reduced in the miR-31 KD embryos (Fig. 1B).

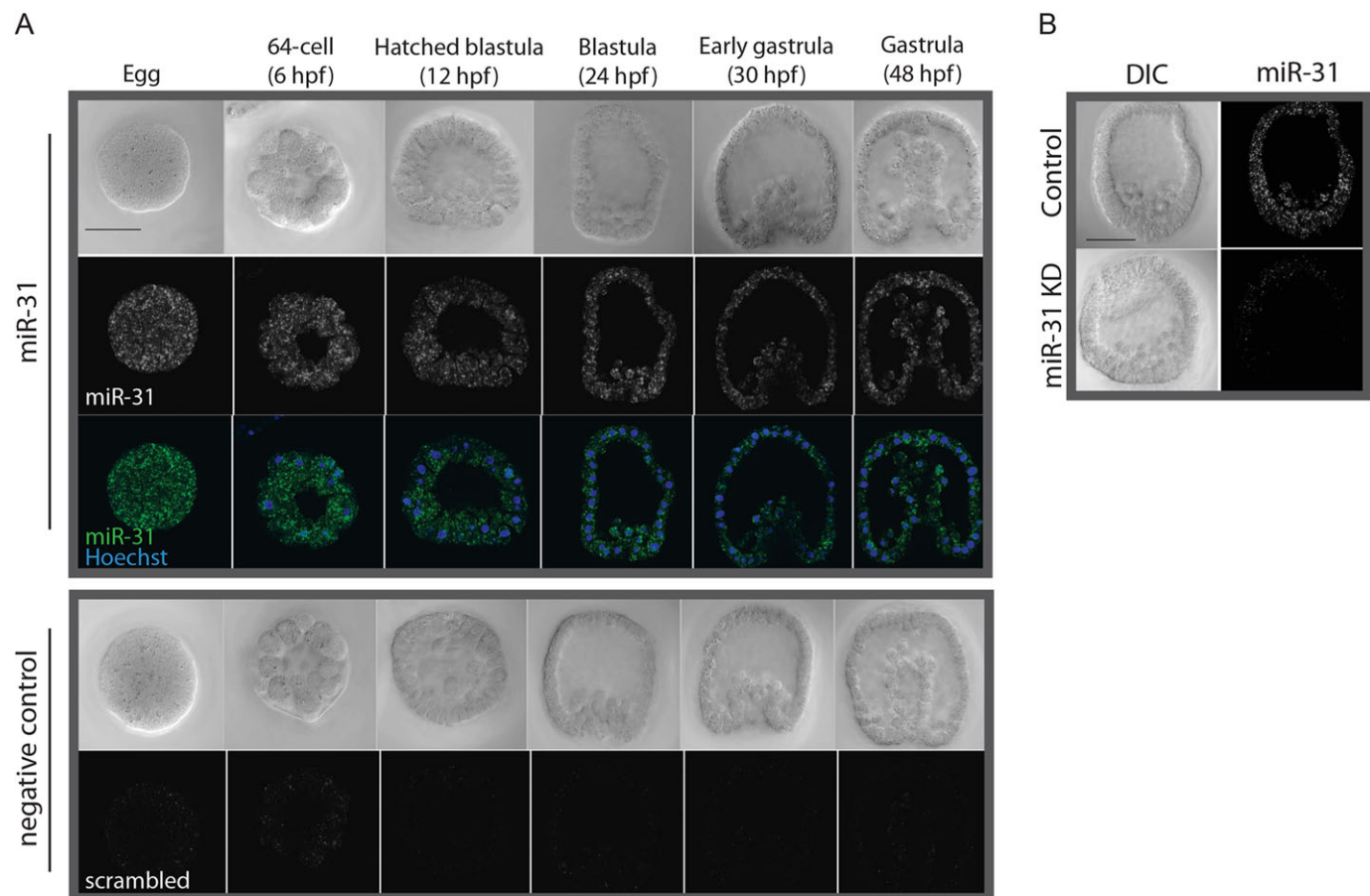


**Fig. 1.** miR-31 is expressed ubiquitously during early development of the sea urchin. Embryos of different developmental stages were labeled by FISH using an LNA probe specific to the mature miR-31 sequence or a scrambled-miR control and counterstained with Hoechst. (A) miR-31 is expressed ubiquitously in the sea urchin embryo. (B) There is a notable decrease in the intensity of miR-31 staining in miR-31 KD blastulae (24 hpf). Scale bar: 50 µm.

### miR-31 KD results in developmental defects

To test the function of miR-31 in the sea urchin embryo, we microinjected miR-31 inhibitor into newly fertilized eggs. The miR-31 inhibitor used for this study is an RNA molecule of complementary sequence to miR-31 that has locked nucleic acid (LNA) monomers incorporated to enhance its affinity to miR-31 and resistance to enzymatic degradation (Naguibneva et al., 2006). The miR-31 inhibitor binds to miR-31 in tight and stable complexes, preventing endogenous miR-31 from binding to its target transcripts (Elmen et al., 2008). Results indicate that miR-31 KD resulted in dose-dependent developmental delay by the mesenchyme blastula stage (24 hpf, Fig. S1). miR-31 KD gastrulae (48 hpf) exhibited a

range of dose-dependent defects, including the formation of cell clumps and extra cells in the blastocoelar space, a reduction in embryo diameter, and a significant decrease in spicule length (Fig. 2). In addition, 7% of the miR-31 KD gastrulae (6 out of 88 embryos, two biological replicates), as opposed to 0% (55 embryos, two biological replicates) of the control gastrulae, developed additional tri-radiate spicule rudiments (Fig. 2D).

Because defects in skeleton spicules may indicate defective PMC patterning, we further examined the spatial distribution of PMCs using the PMC-specific antibody 1D5 (McClay et al., 1983). miR-31 KD PMCs failed to form a ventrolateral ring and failed to migrate anterolaterally (Fig. 3A). The percentage of embryos with

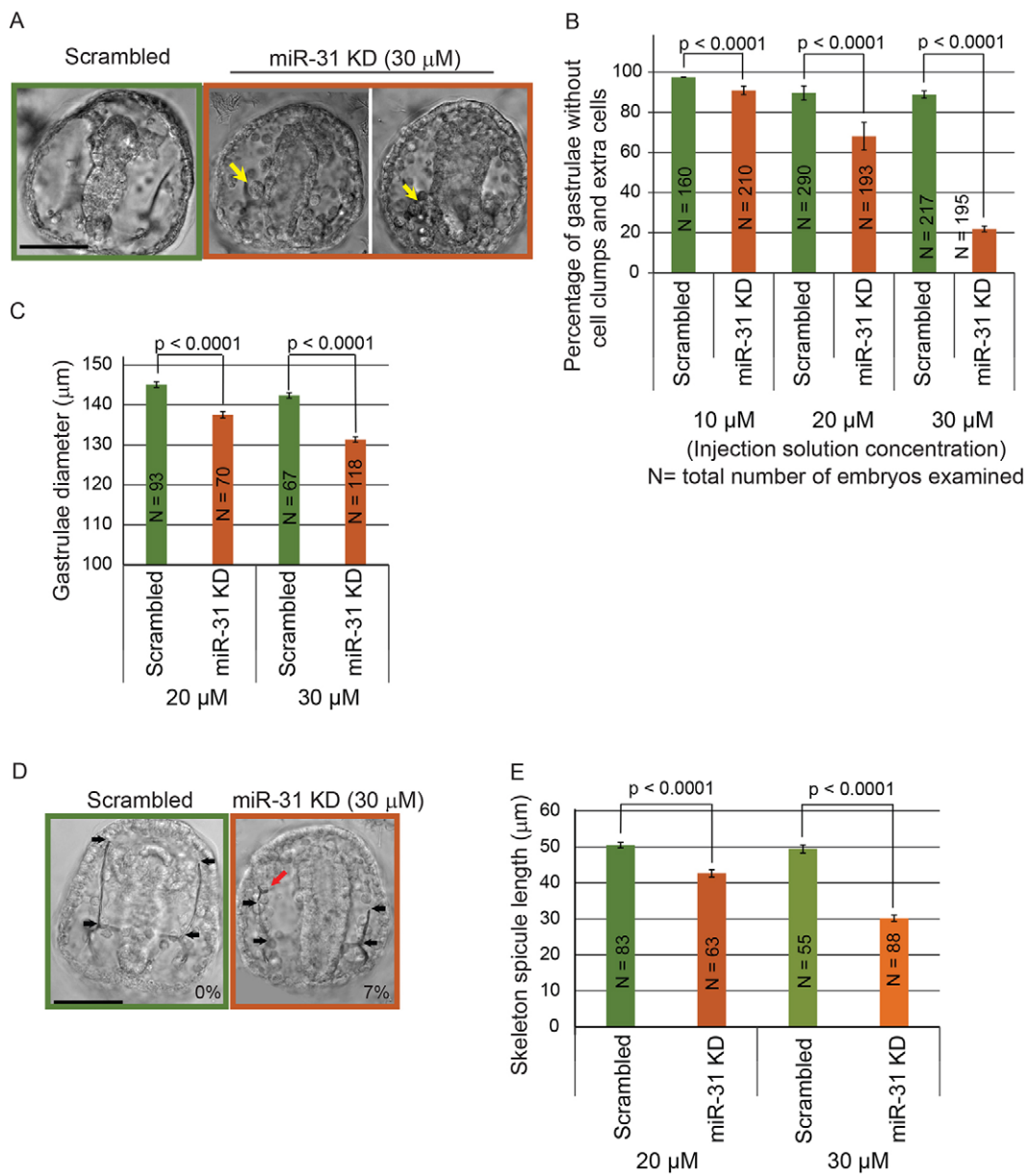


**Fig. 2. miR-31 KD results in dose-dependent developmental defects in sea urchin embryos.** Three concentrations of scrambled negative control or miR-31 LNA inhibitor were microinjected into newly fertilized eggs. (A) miR-31 KD gastrulae exhibited a range of developmental defects. Arrows indicate cell clumps and extra cells in the blastocoelar space. (B) The percentage of embryos with cell clumps and extra cells in the blastocoelar space was dependent on the dose of the miR-31 inhibitor. (C) miR-31 KD gastrulae showed a dose-dependent reduction in embryo diameter, which was determined from the diameter of a circle drawn to include the longest edges of the embryo. (D) The length of skeleton spicules (black arrows) was reduced in miR-31 KD embryos compared with the control. 7% of miR-31 KD embryos contained an extra tri-radiate rudiment at an ectopic location (red arrow). (E) miR-31 KD embryos had a dose-dependent decrease in skeleton spicule length. Student's *t*-test. Error bars indicate s.e.m. Scale bars: 50  $\mu$ m.

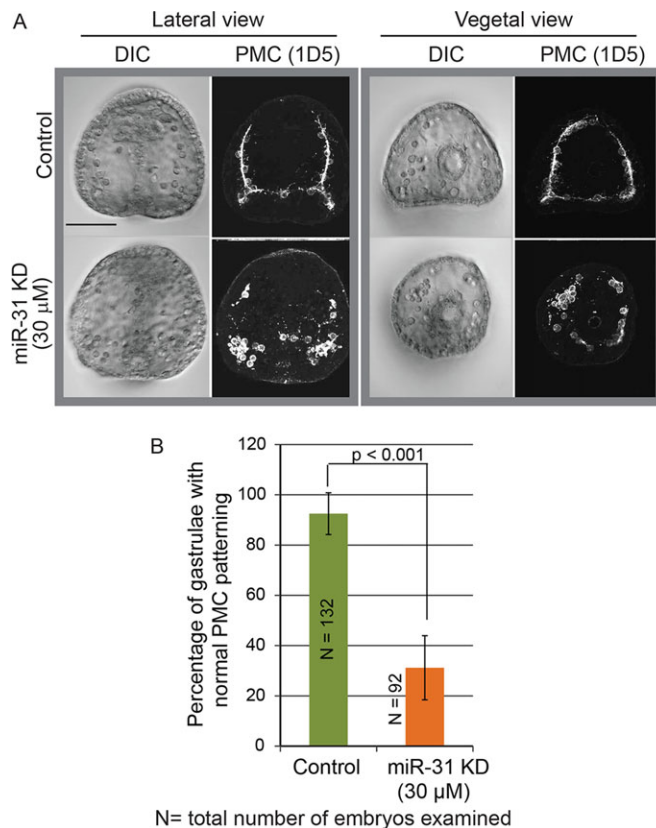


**Fig. 3. miR-31 KD results in skeletogenesis and PMC patterning defects at the gastrula stage.** Embryos were microinjected with miR-31 inhibitor, fixed at gastrula stage, and immunolabeled with 1D5 antibody against PMCs. (A) Inhibition of miR-31 resulted in PMC clumping and failure of the PMCs to migrate anteriorly. (B) The percentage of gastrulae with normal PMC patterning (defined by the proper migration of PMCs towards the animal pole and the lack of mislocalized PMCs and PMC clumps) was significantly reduced in miR-31 KD embryos as compared with the control. Five biological replicates; Cochran-Mantel-Haenszel test; error bars indicate s.e.m. Scale bar: 50  $\mu$ m.

normal PMC patterning (with proper PMC migration, absence of mislocalized PMCs and PMC clumps) was significantly decreased with miR-31 KD in comparison to control embryos (Fig. 3B). To test the specificity of the miR-31 KD phenotype, we supplemented the miR-31 KD embryos with either a miR-31 mimic (Bramsen et al., 2007) or synthetic double-stranded (ds) RNA that corresponds to the miR-31 Dicer substrate (dsRNA-31) (Song et al., 2012). This co-injection significantly rescued the miR-31 KD-induced defects in skeleton spicule length and PMC patterning (Fig. 4, Fig. S2). The miR-31 mimic was more efficient at rescuing the miR-31 KD-induced skeleton spicule defects than dsRNA-31 (63% versus 40%, respectively), as well as at rescuing the miR-31 KD-induced PMC patterning defects (70% versus 46%, respectively). Thus, our results demonstrate that these phenotypes were specific to miR-31 KD.

#### miR-31 directly represses components of the PMC GRN

To determine the molecular mechanism underlying the defects in PMC morphogenesis in miR-31 KD embryos, we performed bioinformatics searches and identified three TFs (*Pmar1*, *Alx1*, *Snail*) and one effector gene (*VegfR7*) within the PMC GRN to have potential miR-31 binding sites within their 3'UTRs (defined by a perfect complementarity to the miR-31 seed sequence) (Fig. 5A). To test whether *Pmar1*, *Alx1*, *Snail* and *VegfR7* are

directly regulated by miR-31, we cloned the 3'UTRs of these genes with wild-type (WT) or mutated miR-31 seed sequences downstream of *Renilla* luciferase (rLuc) reporter constructs (Gregory et al., 2008; Stepicheva et al., 2015) (Fig. 5B). We assayed luciferase construct readouts during a time when the target genes are expressed. Luciferase assays to test direct regulation by miR-31 of *Pmar1* were conducted at the 32-cell stage (6 hpf) and those for *Alx1*, *Snail* and *VegfR7* were conducted at the mesenchyme blastula stage (24 hpf).

Our results indicate that the normalized luciferase signals from rLuc fused with mutated *Pmar1*, *Snail* and *VegfR7* 3'UTRs were significantly increased compared with the signals from rLuc constructs fused with the WT 3'UTRs (Fig. 5C). miRNA binding to the 3'UTR of a target transcript, which would normally silence its translation, would be abolished by mutating the miRNA binding sites, leading to increased translation of luciferase. These data indicated that *Pmar1*, *Snail* and *VegfR7* are suppressed directly by miR-31. The luciferase signals of rLuc constructs containing the *Alx1* 3'UTR with a single mutated miR-31 site did not differ from WT; however, when both miR-31 seed sites in the *Alx1* 3'UTR were mutated the signal from the rLuc construct was significantly increased compared with the WT construct (Fig. 5C). This suggested that the two miR-31 sites within the *Alx1* 3'UTR function redundantly. Of note, the level of increase in luciferase expression observed upon removal of miRNA regulation is consistent with that reported in previous studies (Selbach et al., 2008; Nicolas, 2011; Stepicheva et al., 2015).

All the embryos microinjected with reporter constructs developed normally to the mesenchyme blastula stage, indicating that microinjection of reporter construct mRNAs did not negatively impact embryonic development (Fig. S3A). The mRNA levels of injected luciferase constructs containing WT and mutated miR-31 seed sites of the *Pmar1*, *Alx1* and *VegfR7* 3'UTRs were not significantly different, indicating that the luciferase assays measured post-transcriptional regulation by miR-31 (Fig. S3B).

#### Blockage of miR-31 regulation of *Alx1* and/or *VegfR7* results in aberrant PMC patterning

To test the impact of miR-31 regulation of key genes within the PMC GRN in the dynamic environment of a developing embryo, we designed miR-31 target protector morpholino antisense oligonucleotides (miR-31 TPs) to competitively block endogenous miR-31 suppression of *Alx1* or *VegfR7* (Staton and Giraldez, 2011; Stepicheva et al., 2015). BLASTN of the miR-31 TP sequences indicated that they are uniquely complementary to the functional miR-31 sites identified by the luciferase assays. We microinjected *Alx1* miR-31 TP, *VegfR7* miR-31 TP or both into newly fertilized eggs and observed a significant decrease in the skeleton spicule length compared with control embryos (Fig. 6A,B). A small but significant decrease in skeleton spicule length persisted in *Alx1*, but not in *VegfR7*, miR-31 TP-injected larvae (72 hpf) (Fig. S4). We found that 2%, 7.5% and 4.6% of *Alx1*, *VegfR7* and *Alx1+VegfR7* miR-31 TP-injected gastrulae developed extra tri-radiate rudiments, respectively (Fig. 6A). We also observed that some PMCs were mislocalized in the miR-31 TP-injected embryos compared with the control using the PMC-specific antibody 1D5 (McClay et al., 1983) (Fig. 6C,D). The decrease in skeleton spicule length, formation of the extra tri-radiate rudiments and the defects in PMC patterning (Fig. 6) in the *Alx1* and *VegfR7* miR-31 TP-injected embryos partially mimicked the miR-31 KD phenotypes (Figs 2 and 3), indicating that miR-31 KD phenotypes are in part caused by the lack of miR-31 regulation within PMCs.

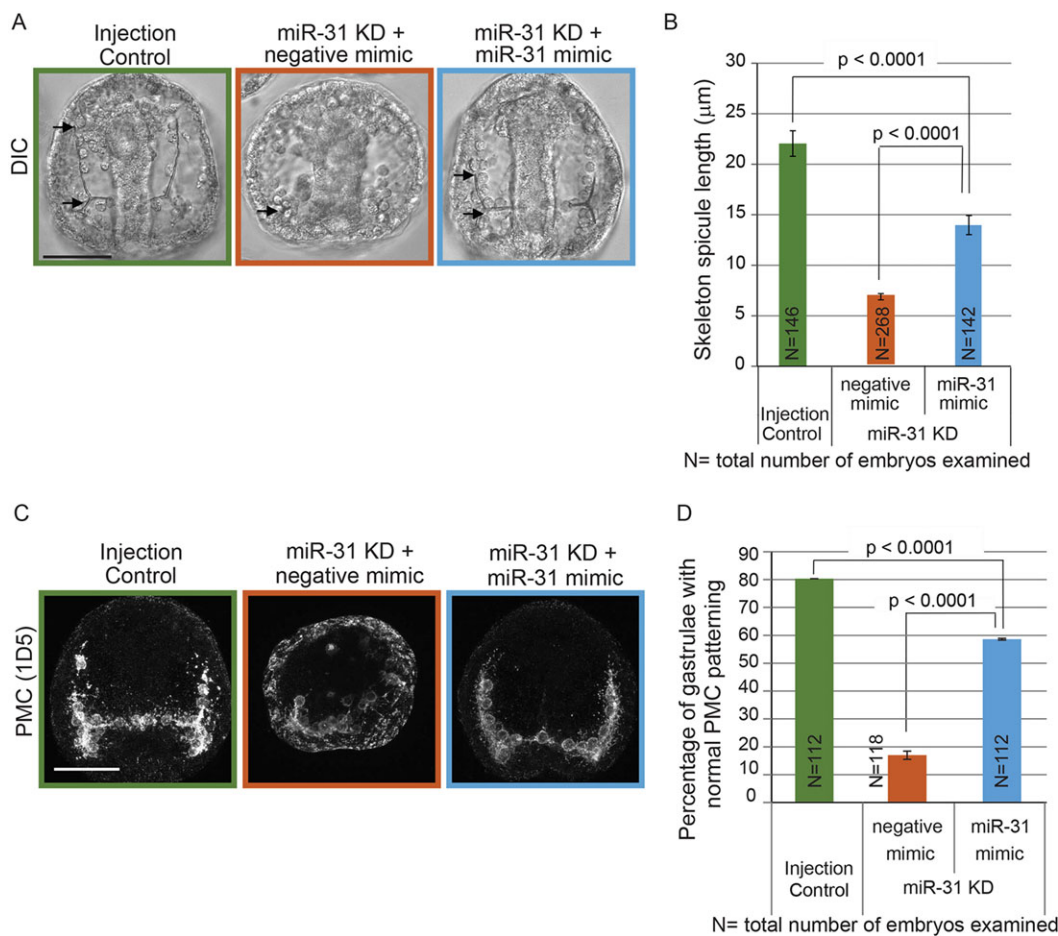


**Fig. 4. miR-31 KD phenotypes are rescued by miR-31 mimics.** (A) Texas Red-dextran (injection control), miR-31 inhibitor with negative control mimic (15 μM each) or miR-31 inhibitor with miR-31 mimic (15 μM each) were microinjected into newly fertilized eggs. Arrows indicate skeleton spicules. (B) The skeleton spicule length in miR-31 KD embryos supplemented with miR-31 mimic was significantly rescued compared with that of miR-31 KD and control embryos (Student's *t*-test). (C) Immunostaining using the PMC-specific antibody 1D5 indicated that the PMC patterning defect in miR-31 KD embryos was rescued by the co-injection of miR-31 inhibitor with the miR-31 mimic. Projection of ten confocal images is shown. (D) PMC patterning defects in miR-31 KD embryos were significantly rescued by the miR-31 mimic. Two biological replicates; Cochran-Mantel-Haenszel test; error bars indicate s.e.m. Scale bars: 50 μm.

#### Mislocalized PMCs in miR-31 KD embryos do not express

##### *VegfR10*

*VegfR10* is the likely receptor to *Vegf3* ligand expressed in the ectoderm, and it has been shown to play a key role in PMC patterning (Lapraz et al., 2006; Duloquin et al., 2007; Adomako-Ankomah and Ettenson, 2013, 2014). We investigated the mechanism of PMC mislocalization by examining the expression of *VegfR10* in the miR-31 KD embryos, as it is also transcriptionally activated by the miR-31 direct target *Alx1* (Rafiq et al., 2012). We used RNA *in situ* hybridization to detect the spatial localization of *VegfR10* transcripts, followed by PMC immunostaining using 1D5 (Fig. 7). Among the miR-31 KD embryos with defective PMC patterning, we found that ~85% of embryos (11 out of 13) that have mislocalized 1D5<sup>+</sup> PMCs also lacked *VegfR10* mRNA expression, compared with 33.3% of control embryos (1 out of 3 embryos with mislocalized PMCs). These results suggested that inhibition of miR-31 results in a subset of PMCs that fail to express *VegfR10* and therefore can not respond to patterning cues (i.e. *Vegf3*) from the ectoderm.

#### miR-31 KD embryos have expanded expression of *Vegf3*

Because miR-31 is expressed in the ectoderm (Fig. 1), we tested whether it regulates *Vegf3* in the ectoderm to impact PMC patterning, using whole-mount *in situ* hybridization and qPCR to

determine the spatial distribution and level, respectively, of *Vegf3* expression in miR-31 KD and control embryos (Figs 8 and 9). The expression of *Vegf3* in the mesenchyme blastulae was expanded in the ectoderm and shifted anteriorly, indicating that miR-31 regulates *Vegf3* expression (Fig. 8). We also observed an average 1.6-fold increase in *Vegf3* transcripts in miR-31 KD embryos compared with the control (Fig. 9). Because we did not find miR-31 seed sequence within the *Vegf3* mRNA, regulation of *Vegf3* by miR-31 is likely to be indirect. Thus, miR-31 regulates both the signal-receiving PMCs and the signal-sending cells in the ectoderm to mediate proper *Vegf* signaling that impacts PMC patterning.

#### miR-31 KD results in changes in the mRNA levels of several genes

To test the regulatory effect of miR-31 on its direct and indirect targets at the transcriptional level, we compared the mRNA levels of its direct targets (*Pmar1*, *Alx1*, *Snail* and *VegfR7*) and genes involved in PMC patterning (*FGF*, *Vegf3*, *VegfR7*) in control and miR-31 KD embryos (Fig. 9). mRNA levels were assayed at the early blastula stage, when all the identified direct miR-31 targets are expressed. Results indicated that most of the miR-31 targets were not altered upon miR-31 KD. However, we observed an average 2.2-fold and 1.6-fold accumulation of *VegfR7* and *Vegf3* mRNAs,

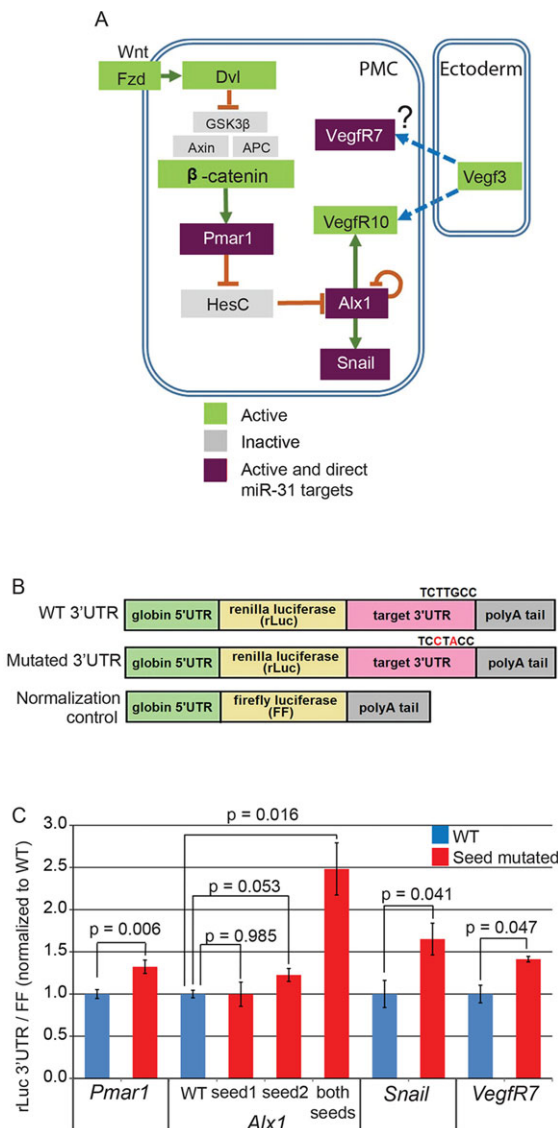


**Fig. 5.** miR-31 directly represses several genes within the skeletogenic GRN. (A) Simplified PMC GRN indicating that PMCs are specified by the Wnt/ $\beta$ -catenin signalling pathway, which activates the transcriptional repressor *Pmar1* in the vegetal pole of the embryo. *Pmar1* activation inhibits the transcription of *HesC*, leading to the activation of skeletogenic TFs such as *Alx1*. *Alx1* activates skeletogenic effector genes, including *Snail* and *VegfR10*. The 3'UTRs of *Pmar1*, *Alx1*, *Snail* and *VegfR7* contain miR-31 seed sequences (purple). (B) The 3'UTRs of potential miR-31 targets were fused downstream of *Renilla* luciferase (rLuc). Site-directed mutagenesis was used to mutate miR-31 seed sequences. Firefly luciferase (FF) flanked with *Xenopus*  $\beta$ -globin UTRs was used for normalization. (C) Luciferase readings from embryos injected with constructs containing mutated miR-31 binding sites of *Pmar1*, *Alx1*, *Snail* and *VegfR7* 3'UTRs were increased significantly in comparison to embryos injected with constructs containing the WT miR-31 seed sites, indicating that miR-31 directly represses these genes. Three to six biological replicates; Student's *t*-test; error bars indicate s.e.m.

respectively, in the miR-31 KD embryos compared with the control, indicating that miR-31 is able to induce the degradation of *VegfR7* and *Vegf3* transcripts or that the absence of miR-31 causes their increased expression.

## DISCUSSION

We used the sea urchin as a model to examine the function of miR-31 in early embryogenesis and revealed that it regulates various

aspects of PMC development. The loss of miR-31 resulted in significantly shorter spicules, the formation of additional tri-radiate rudiments, and PMC patterning defects. We identified that miR-31 suppresses components of the PMC GRN and also *Vegf3* expression in the ectoderm to regulate proper PMC patterning and function.

miR-31 is a highly evolutionarily conserved miRNA that plays a role in cancer and bone homeostasis in vertebrates; however, the function of miR-31 has not been well defined in the developing embryo (Aboobaker et al., 2005; Wienholds et al., 2005; Valastyan and Weinberg, 2010; Yamagishi et al., 2012; Baglio et al., 2013; Deng et al., 2013a,b; Xu et al., 2013). Previously, we identified miR-31 as highly expressed in the early sea urchin embryo, and miR-31 was one of the four miRNAs that was needed to rescue the developmental defects induced by KD of the key miRNA processing enzyme Drosha, indicating the potentially important role of miR-31 in early development (Song et al., 2012).

miR-31 is ubiquitously expressed in zebrafish embryos (Wienholds et al., 2005). It is also expressed in a pair-rule pattern in the foregut, anterior endoderm and hindgut of the *Drosophila* embryo (Aboobaker et al., 2005). Similar to zebrafish, miR-31 expression is ubiquitous in the sea urchin embryo; however, it localizes to punctate structures that do not appear to be nuclear, a pattern that was found typical for only a few miRNAs, such as miR-34b, in zebrafish embryos, and for a number of dendritic or axonic miRNAs, such as miR-26a, miR-124a, pre-miR-25 and pre-miR-433, in rats (Kye et al., 2007; Wang et al., 2013; Goldie et al., 2014; Kim et al., 2015). miRNAs or pre-miRNAs that show punctate localization in dendrites or axons are thought to be compartmentalized to perform localized activity-dependent translation (Goldie et al., 2014; Kim et al., 2015). Further study is required to identify the nature of the punctate pattern of miR-31 in the sea urchin embryo.

miR-31 KD embryos exhibit various skeletogenic defects (Fig. 2D and Fig. 3). PMC patterning and the formation of connecting syncytia are requisite for spiculogenesis, since PMCs deposit calcite within the syncytium space that acts as a mold (Wilt, 1999, 2002; Lyons et al., 2014; Vidavsky et al., 2014). However, other factors may control the expression of biominerization genes needed for skeletogenesis later in development (Rafiq et al., 2012; Sun and Ettensohn, 2014). Thus, the PMC patterning defects in the miR-31 KD embryos may contribute in part to the shortening of the skeleton spicules (Fig. 2E) and miR-31 may also regulate biominerization genes. In addition, recombinant sea urchin *Vegf3* was found to be crucial in directing single calcite crystal growth and skeleton branching in an *in vitro* system, such that a low *Vegf3* concentration (5  $\mu$ g/ml) induced the formation of linear spicules whereas a high *Vegf3* concentration (30–150  $\mu$ g/ml) induced tri-radiate rudiment formation (Knapp et al., 2012). We found that miR-31 KD embryos have increased expression of *Vegf3* in the ectoderm, and the increased *Vegf3* might contribute to the formation of additional tri-radiate rudiments.

miR-31 exerts a relatively small but significant suppression of multiple targets within the PMC GRN that is sufficient to impact PMC patterning and function (Figs 5, 6 and 9). Thus, miR-31 is similar to other miRNAs that act as ‘fine-tuners’, such that effects on individual target genes are usually small (Selbach et al., 2008). However, a single miRNA can power developmental decisions. For example, miRNAs may sharpen morphogen gradients in the developing embryo (Niehrs, 2004; Martello et al., 2007) and they can also serve as a positive regulator by amplifying signal strength in duration to allow cells to respond to subthreshold stimuli (Meng et al., 2007; Fish et al., 2008; Kuhnert et al., 2008; Thum et al.,

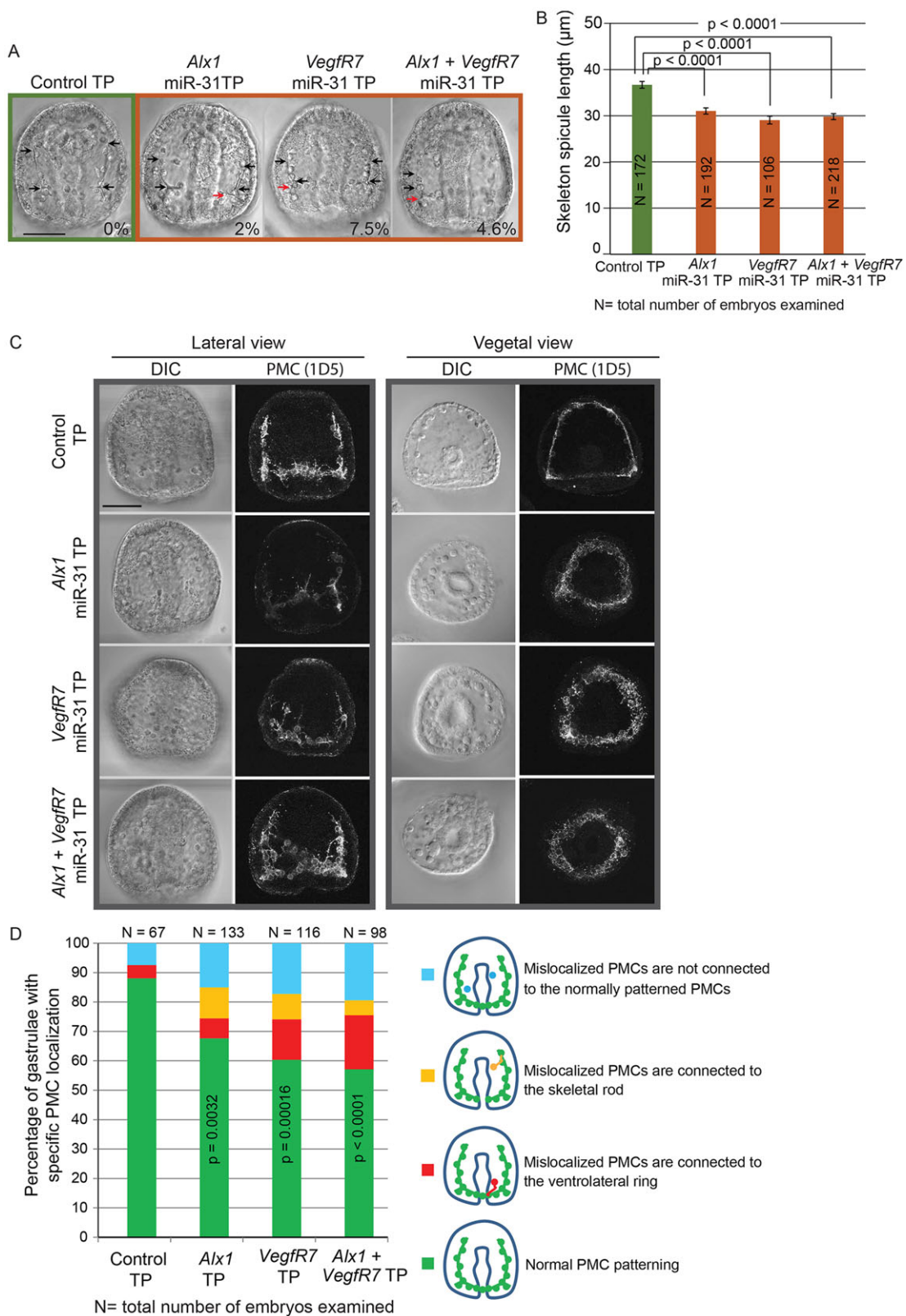


**Fig. 6. Removal of miR-31 regulation of *Alx1* and *VegfR7* disrupts skeletogenesis and PMC patterning.** Control TPs and miR-31 TPs (designed to specifically block functional miR-31 binding sites within *Alx1* and *VegfR7* 3'UTRs) were microinjected into newly fertilized eggs and collected at the gastrula stage. (A) Microinjection of *Alx1* and/or *VegfR7* miR-31 TPs resulted in shortening of the skeleton spicules (black arrows) and formation of an extra tri-radiate rudiment at ectopic locations (red arrows). The percentage of gastrulae displaying an extra tri-radiate is indicated. (B) The length of skeleton spicules extending anteriorly was significantly decreased in the presence of *Alx1*, *VegfR7* or *Alx1+VegfR7* miR-31 TPs compared with the control. One-way ANOVA; error bars indicate s.e.m. (C) The presence of miR-31 TPs resulted in mislocalization of PMCs. (D) The percentage of embryos with normal PMC localization was significantly decreased in the presence of miR-31 TPs compared with the control. Fisher's exact test of independence. Scale bars: 50 μm.

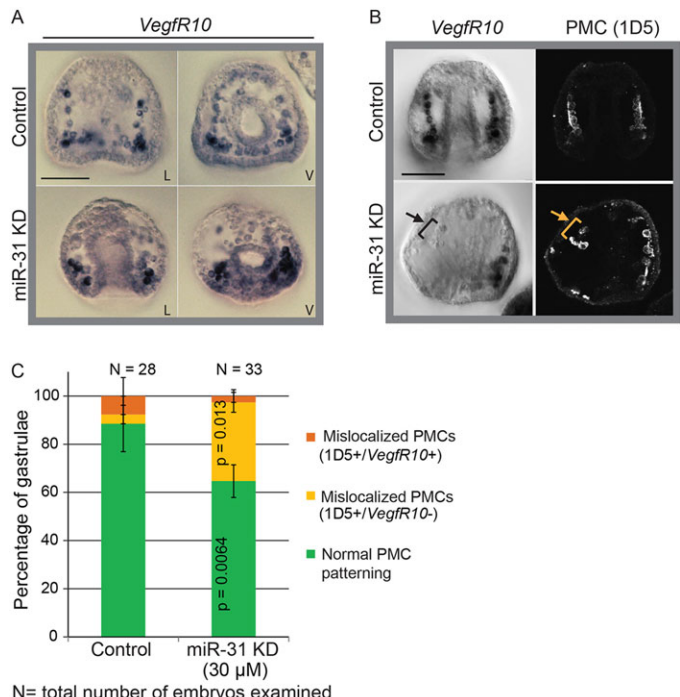


**Fig. 7. Mislocalized PMCs in miR-31 KD embryos do not express *VegfR10*.**  
Whole-mount RNA *in situ* hybridization (WMISH) against *VegfR10* was performed in miR-31 KD and control gastrulae. L, lateral; V, ventral.  
(A) *VegfR10* was most strongly expressed in the PMCs located close to the vegetal pole of miR-31 KD embryos. (B) Mislocalized 1D5-immunopositive PMCs in miR-31 KD embryos do not express *VegfR10* (arrows). (C) The percentage of embryos with normal PMC patterning was significantly reduced in miR-31 KD gastrulae compared with the control. The percentage of embryos in which mislocalized PMCs did not express *VegfR10* was significantly increased in miR-31 KD gastrulae as compared with the control (32.7% 1D5<sup>+</sup> *VegfR10*<sup>-</sup>). Cochran-Mantel-Haenszel test; error bars indicate s.e.m.  
Scale bars: 50 µm.

2008; Inui et al., 2010). In this manner, miR-31 might precisely and promptly fine-tune gene expression thresholds that are important within the developmental pathway or GRN of PMCs to ensure their proper development and function.

Our experiments using miR-31 TPs demonstrated that miR-31 regulation of *Alx1* (an upstream regulator of *VegfR10*) and/or *VegfR7* is important for proper PMC patterning (Fig. 6). Embryos with combined *Alx1* and *VegfR7* miR-31 TP treatment exhibited more severe PMC patterning defects than those treated with the single *Alx1* or *VegfR7* miR-31 TP, indicating that miR-31 targets both genes independently. The miR-31 TP effects decreased by the larval stage, suggesting that the miR-31 TP-treated embryos overcome the lack of miR-31 inhibition by other regulatory mechanisms. In addition, the increased severity of the phenotypes observed in miR-31 KD embryos (Figs 2 and 3) in comparison to *Alx1* and *VegfR7* miR-31 TP-treated embryos (Fig. 6) indicates that miR-31 also targets other unidentified genes, which cumulatively leads to the more severe PMC defects.

Interestingly, we found that the majority of mislocalized PMCs in miR-31 KD embryos lack *VegfR10* expression (Fig. 7). The molecular mechanism of this *VegfR10* downregulation still needs to be determined. The mislocalized PMCs lacking *VegfR10* might fail to receive the *Vegf3* signal that is required to pattern correctly. This also demonstrates that miR-31 exerts variable levels of suppression of *VegfR10* and/or that local factors modulate *VegfR10* expression to impact the directed migration of PMCs.

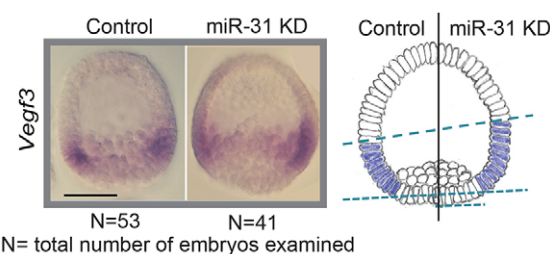


**Fig. 8. miR-31 KD results in expansion of the *Vegf3* expression domain in the ectoderm.** WMISH against *Vegf3* was performed in miR-31 KD and control blastula stage embryos. The expression of *Vegf3* was expanded and anteriorly shifted in miR-31 KD embryos as compared with the control. Scale bar: 50 µm.

Our results demonstrate that miR-31 also regulates *Vegf3* expression in the ectoderm. miR-31 KD embryos have expanded and increased expression of *Vegf3* as indicated by *in situ* hybridization and qPCR data (Figs 8 and 9). *Vegf3* is selectively activated in the BE, an ectoderm-endoderm boundary that is specified through short-range Wnt5 signaling (Wnt5 is a ligand for non-canonical Wnt signaling) from the endoderm (Slusarski et al., 1997; McIntyre et al., 2013). Early in development *Vegf3* is expressed broadly across the BE, and by the blastula stage it becomes restricted to the two lateral patches by TGFβ signaling (McIntyre et al., 2013). Thus, *Vegf3* expression is regulated both by non-canonical Wnt signaling in the anterior/posterior axis and by TGFβ signaling mediated by Nodal and Bmp2/4 in the oral/aboral axis. Our data indicated that *Vegf3* expression is expanded anteriorly and not along the oral/aboral axis in miR-31 KD embryos, suggesting that miR-31 might be regulating non-canonical Wnt signaling and thus indirectly regulating *Vegf3* expression (Figs 8 and 9).

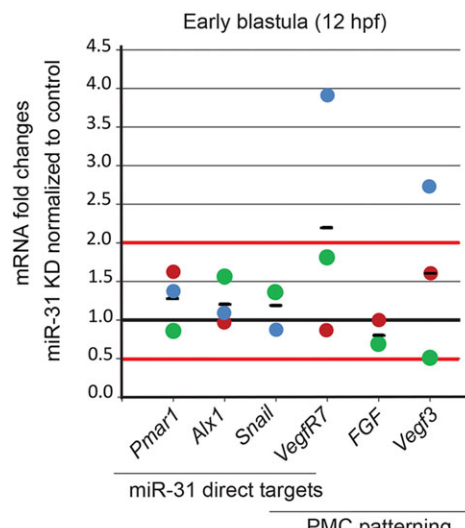


**Fig. 9. *VegfR7* and *Vegf3* transcripts accumulate in miR-31 KD embryos.**  
The transcript levels of direct miR-31 targets and of genes involved in PMC patterning and movement were measured in miR-31 KD and control embryos at early blastula stage (12 hpf), prior to visible morphological defects. qPCR analysis revealed the accumulation of *VegfR7* and *Vegf3* mRNA in miR-31 KD embryos. Data are normalized to the *ubiquitin* internal control and presented as fold change of transcripts in miR-31 KD embryos normalized to the control embryos. Each colored dot represents an independent biological replicate, with the black bar representing the average. Horizontal red lines mark 2-fold level changes.

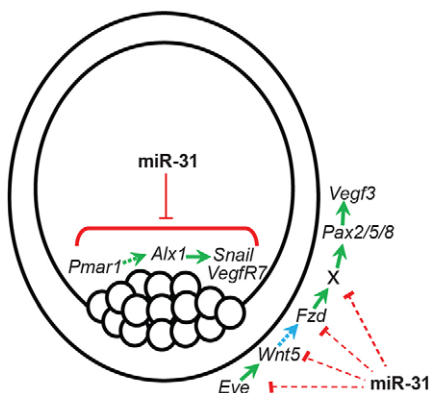


**Fig. 10. Model of miR-31 regulation in PMC patterning and function.** miR-31 directly suppresses several key components within the PMC GRN: *Pmar1*, *Alx1*, *Snail* and *VegfR7*. *Eve* activates transcription of *Wnt5* in the endoderm; *Wnt5* then acts as a short-range signaling molecule to *Fzd* expressed in the ectoderm. Activation of the non-canonical Wnt pathway in the ectoderm turns on an unidentified activator (X) that transcriptionally activates *Pax2/5/8*, leading to *Vegf3* transcription. The model predicts that miR-31 also regulates ectodermally derived PMC patterning signals, potentially through its regulation of activators, components and/or genes downstream of the non-canonical Wnt pathway. miR-31 coordinately regulates genes within the PMCs and in the ectoderm to ensure proper PMC patterning and function.

The cognate Frizzled (Fzd) receptor of Wnt5 has not been identified. However, Fzd9/10 may be a potential receptor for Wnt5, as their expression domains overlap (Cui et al., 2014). Using a bioinformatics approach, we identified a truncated miR-31 seed sequence within the 3'UTRs of *Wnt5* and *Fzd9/10* and a complete miR-31 seed sequence within the 3'UTRs of *Fzd5/8* and *Eve* (Even-skipped), indicating that these genes are predicted targets of miR-31. *Eve* is a homeodomain TF that was recently shown to regulate the expression of *Wnt5* in endodermal cells (Cui et al., 2014). In addition, an as yet unidentified factor is responsible for activating *Pax2/5/8*, which in turn activates *Vegf3* expression (Rottinger et al., 2008; McIntyre et al., 2013). Thus, miR-31 may directly suppress the activators, components or genes downstream of the non-canonical Wnt pathway to indirectly regulate the expression of *Vegf3* in the ectoderm (Fig. 10). These results indicate that, in addition to targeting multiple genes within the PMC GRN, miR-31 might also cross-regulate Vegf and non-canonical Wnt signaling pathways to impact PMC patterning.

In summary, our study revealed the novel function of miR-31 in regulating PMC patterning by directly suppressing several key targets within the PMC GRN and indirectly suppressing *Vegf3* in the ectoderm. miR-31 is known to negatively regulate vertebrate lymphatic vascular lineage differentiation and development, a process that involves directed cell migration in response to external signals and that is analogous to PMC patterning (Pedrioli et al., 2010). The role of miR-31 in regulating PMC patterning in response to Vegf signaling in the invertebrate sea urchin indicates its conserved function in development. In the future, it will be interesting to examine further the molecular mechanism of miR-31 cross-regulation of components of the non-canonical Wnt and Vegf signaling pathways.

## MATERIALS AND METHODS

### Animals

Adult *Strongylocentrotus purpuratus* were obtained from Point Loma Marine Company (San Diego, CA, USA) and maintained in an aquarium tank containing artificial sea water (Instant Ocean) at 15°C. Gametes were obtained by intracoelomic injection of 0.5 M KCl and embryos were

cultured at 15°C in filtered natural sea water collected from the Indian River Inlet (University of Delaware, Lewes, DE, USA).

### Microinjections

Microinjections were performed as described previously (Cheers and Ettensohn, 2004; Stepicheva and Song, 2014). All injection solutions contained 20% sterile glycerol and 2 mg/ml 10,000 MW Texas Red lysine-charged dextran (Molecular Probes) to mark the microinjected embryos. The volume of the injected solution was calculated to be 1–2 pl based on the size of the injection bolus at about one-fifth of the egg diameter. The microinjected miR-31 inhibitor (Cel-miR-72) and the scrambled negative control A (miRCURY LNA power inhibitor, Exiqon) were estimated to be ~34.5 attomoles (from the 30 μM injection stock solution). The miR-31 mimic (Hsa-miR-31-5p) contains miR-31 RNA complexed with two LNA-modified RNA strands that simulate naturally occurring mature miRNAs and reduce off-target effects from segmented passenger strands (Bramsen et al., 2007). Cel-miR-39-3p (Exiqon) was used as the negative control mimic. The miR-31 mimic or dsRNA-31 [Dicer substrate of miR-31 (Song et al., 2012)] was co-injected with a miR-31 inhibitor at a 1:1 molar ratio to test the specificity of miR-31 KD.

miRNA target protector (TP) morpholinos were designed against miR-31 binding sites identified by dual-luciferase assays and site-directed mutagenesis (GeneTools) (Table S2). The control morpholino does not recognize sea urchin genes (as assessed by BLASTN). The concentration of each miR-31 TP in the microinjection solution was 3 μM, which was empirically determined to result in defective phenotypes.

### Immunofluorescence

Immunolabeling with 1D5 antibody (McClay et al., 1983) was performed as described previously with modifications. The microinjected gastrulae were collected and fixed in 4% paraformaldehyde (Electron Microscopy Sciences) in artificial sea water for 30 min or overnight followed by four 10-min washes with PBS-Tween [PBS containing 0.05% Tween 20 (Bio-Rad)]. As a blocking solution, 4% goat serum in PBS-Tween was added for 1 h at room temperature, followed by overnight incubation with 1D5 primary antibody at 1:50 dilution. Embryos were then washed four times for 10 min each with PBS-Tween followed by 1 h incubation with goat anti-mouse Alexa Fluor 488-conjugated secondary antibody (Invitrogen, A11001) at 1:300.

### Whole-mount *in situ* hybridization

*VegfR10* and *Vegf3* genes were PCR amplified from sea urchin embryonic cDNA and cloned into Zero-Blunt (Invitrogen) to generate RNA *in situ* probes (PCR primers are listed in Table S1). RNA *in situ* probes were synthesized with the Anti-Digoxigenin-AP Labeling Kit (Roche Diagnostics). 1 ng/μl mRNA was used to detect native transcript in embryos (Minokawa et al., 2004; Stepicheva et al., 2015). Images were acquired with a Zeiss Observer Z1 microscope and Nikon D90 digital camera.

miR-31 (Cel-miR-72 miRCURY LNA detection probe) and negative control scrambled-miR LNA detection probes (Exiqon) were used in FISH as described previously with modifications (Sethi et al., 2014). Pre-hybridization was performed in hybridization buffer containing 70% formamide for 3 h at 50°C (without the equilibration steps). Embryos were incubated with 0.1 ng/μl miR-31 or scrambled-miR negative control probes for 4 days at 50°C followed by MOPS buffer washes, blocking and incubation with Anti-Digoxigenin-POD Fab fragments (Roche Diagnostics). The TSA-Plus Fluorescein System (PerkinElmer) was used to detect the fluorescence signal. The embryos were counterstained with Hoechst 33342 (Lonza) at 1:1000 dilution for 5 min followed by three 10-min PBS-Tween washes. Images were acquired with a Zeiss LSM 780 confocal microscope.

### Real-time quantitative PCR (qPCR)

One-hundred microinjected embryos were collected at the hatched blastula stage (12 hpf) and total RNA extracted using the Micro RNeasy Kit (Qiagen). cDNA was synthesized using the iScript cDNA Synthesis Kit

(Bio-Rad). qPCR was performed using two embryo-equivalents for each reaction using Power SYBR Green PCR Master Mix (Invitrogen) in the 7300 real-time PCR cycler system (Applied Biosystems) as previously described (Stepicheva et al., 2015). Primers were designed using the Primer3 program (Rozen and Skaletsky, 2000) (Table S3).

### Cloning 3'UTRs into luciferase reporter constructs

The 3'UTR of *Pmar1* was obtained using the First Choice RLM-RACE Kit (Invitrogen) using *Pmar1\_RACE\_F1* and *Pmar1\_RACE\_F2* primers (Table S1). PCR primers of 3'UTR sequences of *Alx1*, *VegfR7* and *Snail* were designed based on sequence information available from the sea urchin genome (echinobase.org) (Table S1). The amplified PCR products for the 3'UTRs were cloned into PCRII or Zero-Blunt vectors (Invitrogen). Bacterial colonies containing potential PCR inserts were sequenced by Genewiz Services (South Plainfield, NJ, USA) to validate sequences.

We generated the *Renilla* luciferase vector (rLuc) by PCR amplification of the rLuc coding sequence from the psiCHECK dual-luciferase vector (Promega). This rLuc PCR fragment was cloned into the pSP6T4 vector (Gustafson and Wessel, 2010) to generate SupLuc. 3'UTRs from positive clones were excised from the PCRII or Zero-Blunt vectors using *Xba*I/*Not*I double digests and gel purified with the Wizard SVgel and PCR Cleanup Kit (Promega). *Pmar1*, *Snail* and *VegfR7* 3'UTRs were ligated with the SupLuc vector, and the *Alx1* 3'UTR was ligated with the psiCHECK vector directly. Firefly luciferase construct was prepared and used as an injection control as described previously (Stepicheva et al., 2015).

### Site-directed mutagenesis

The miR-31 seed sequence (5'-TCTTGCC-3') within the 3'UTRs of target genes was mutated at positions 3 and 5 (5'-TCTACC-3') to disrupt miR-31 target binding (Gregory et al., 2008; Stepicheva et al., 2015). Mutations were generated using the QuikChange Lightning Kit (Agilent Technologies). Clones were sequenced to confirm the presence of miR-31 binding site mutations (Genewiz Services). Primers are listed in Table S1.

### In vitro transcription

All SupLuc-based reporter constructs were linearized with *Eco*RI and *in vitro* transcribed with SP6 RNA polymerase using the mMESSAGE mMACHINE Kit (Ambion). The *Alx1* 3'UTR in psiCHECK was linearized with *Not*I and *in vitro* transcribed with T7 RNA polymerase. Firefly luciferase (FF) was linearized using *Spe*I and *in vitro* transcribed with SP6 RNA polymerase. mRNAs were purified using the Micro RNeasy Kit, followed by an additional purification step on a spin column (Millipore, UFC30GV0S) prior to injection.

### Dual-luciferase quantification

The injection solutions for the dual-luciferase assay contained 20% sterile glycerol, 2 mg/ml 10,000 MW Texas Red lysine-charged dextran, 60 ng/μl FF mRNA and 4 ng/μl (*Pmar1* constructs) or 40 ng/μl (*Alx1* constructs) rLuc mRNA. 20–30 embryos were collected at select time points and processed as previously described (Stepicheva et al., 2015). The rLuc signal in each sample was normalized to the FF signal to account for microinjection volume differences and the data were normalized to the WT reporter construct expression.

### Acknowledgements

We thank Dr David McClay (Duke University) for the generous gift of 1D5 antibody.

### Competing interests

The authors declare no competing or financial interests.

### Author contributions

N.A.S. performed the experiments. N.A.S. and J.L.S. wrote the paper.

### Funding

This work was supported by the University of Delaware start-up fund to J.L.S. and a grant from NIH/NIGMS [1P20GM10365301A]. Deposited in PMC for release after 12 months.

### Supplementary information

Supplementary information available online at <http://dev.biologists.org/lookup/suppl/doi:10.1242/dev.127969/-DC1>

### References

- Aboobaker, A. A., Tomancak, P., Patel, N., Rubin, G. M. and Lai, E. C. (2005). Drosophila microRNAs exhibit diverse spatial expression patterns during embryonic development. *Proc. Natl. Acad. Sci. USA* **102**, 18017–18022.
- Adomako-Ankomah, A. and Ettensohn, C. A. (2013). Growth factor-mediated mesodermal cell guidance and skeletogenesis during sea urchin gastrulation. *Development* **140**, 4214–4225.
- Adomako-Ankomah, A. and Ettensohn, C. A. (2014). Growth factors and early mesoderm morphogenesis: insights from the sea urchin embryo. *Genesis* **52**, 158–172.
- Augoff, K., Das, M., Bialkowska, K., McCue, B., Plow, E. F. and Sossey-Alaoui, K. (2011). miR-31 is a broad regulator of beta 1-integrin expression and function in cancer cells. *Mol. Cancer Res.* **9**, 1500–1508.
- Baglio, S. R., Devescovи, V., Granchi, D. and Baldini, N. (2013). MicroRNA expression profiling of human bone marrow mesenchymal stem cells during osteogenic differentiation reveals Osterix regulation by miR-31. *Gene* **527**, 321–331.
- Bartel, D. P. (2009). MicroRNAs: target recognition and regulatory functions. *Cell* **136**, 215–233.
- Batlle, E., Sancho, E., Franci, C., Domínguez, D., Monfar, M., Baulida, J. and García De Herreros, A. (2000). The transcription factor snail is a repressor of E-cadherin gene expression in epithelial tumour cells. *Nat. Cell Biol.* **2**, 84–89.
- Bramsen, J. B., Laursen, M. B., Damgaard, C. K., Lena, S. W., Ravindra Babu, B., Wengel, J. and Kjems, J. (2007). Improved silencing properties using small internally segmented interfering RNAs. *Nucleic Acids Res.* **35**, 5886–5897.
- Cheers, M. S. and Ettensohn, C. A. (2004). Rapid microinjection of fertilized eggs. *Methods Cell Biol.* **74**, 287–310.
- Cui, M., Siriwon, N., Li, E., Davidson, E. H. and Peter, I. S. (2014). Specific functions of the Wnt signalling system in gene regulatory networks throughout the early sea urchin embryo. *Proc. Natl. Acad. Sci. USA* **111**, E5029–E5038.
- Damle, S. and Davidson, E. H. (2011). Precise cis-regulatory control of spatial and temporal expression of the alx-1 gene in the skeletogenic lineage of *S. purpuratus*. *Dev. Biol.* **357**, 505–517.
- Dee, C. T., Szymoniuk, C. R., Mills, P. E. D. and Takahashi, T. (2013). Defective neural crest migration revealed by a zebrafish model of Alx1-related frontonasal dysplasia. *Hum. Mol. Genet.* **22**, 229–251.
- Deng, Y., Zhou, H., Zou, D., Xie, Q., Bi, X., Gu, P. and Fan, X. (2013a). The role of miR-31-modified adipose tissue-derived stem cells in repairing rat critical-sized calvarial defects. *Biomaterials* **34**, 6717–6728.
- Deng, Y., Wu, S., Zhou, H., Bi, X., Wang, Y., Hu, Y., Gu, P. and Fan, X. (2013b). Effects of a miR-31, Runx2, and Satb2 regulatory loop on the osteogenic differentiation of bone mesenchymal stem cells. *Stem Cells Dev.* **22**, 2278–2286.
- Deng, Y., Zhou, H., Gu, P. and Fan, X. (2014a). Repair of canine medial orbital bone defects with miR-31-modified bone marrow mesenchymal stem cells. *Invest. Ophthalmol. Vis. Sci.* **55**, 6016–6023.
- Deng, Y., Bi, X., Zhou, H., You, Z., Wang, Y., Gu, P. and Fan, X. (2014b). Repair of critical-sized bone defects with anti-miR-31-expressing bone marrow stromal stem cells and poly(glycerol sebacate) scaffolds. *Eur. Cell. Mater.* **27**, 13–24; discussion 24–25.
- Duboc, V., Lapraz, F., Saudemont, A., Bessodes, N., Mekpoh, F., Haillot, E., Quirin, M. and Lepage, T. (2010). Nodal and BMP2/4 pattern the mesoderm and endoderm during development of the sea urchin embryo. *Development* **137**, 223–235.
- Duloquin, L., Lhomond, G. and Gache, C. (2007). Localized VEGF signaling from ectoderm to mesenchyme cells controls morphogenesis of the sea urchin embryo skeleton. *Development* **134**, 2293–2302.
- Dunworth, W. P., Cardona-Costa, J., Bozkulak, E. C., Kim, J.-D., Meadows, S., Fischer, J. C., Wang, Y., Cleaver, O., Qyang, Y., Ober, E. A. et al. (2014). Bone morphogenetic protein 2 signaling negatively modulates lymphatic development in vertebrate embryos Novelty and Significance. *Circ. Res.* **114**, 56–66.
- Elmen, J., Lindow, M., Silahtaroglu, A., Bak, M., Christensen, M., Lind-Thomsen, A., Hedtjarn, M., Hansen, J. B., Hansen, H. F., Straarup, E. M. et al. (2008). Antagonism of microRNA-122 in mice by systemically administered LNA-antimiR leads to up-regulation of a large set of predicted target mRNAs in the liver. *Nucleic Acids Res.* **36**, 1153–1162.
- Ettensohn, C. A., Illies, M. R., Oliveri, P. and De Jong, D. L. (2003). Alx1, a member of the Cart1/Alx3/Alx4 subfamily of Paired-class homeodomain proteins, is an essential component of the gene network controlling skeletogenic fate specification in the sea urchin embryo. *Development* **130**, 2917–2928.
- Fish, J. E., Santoro, M. M., Morton, S. U., Yu, S., Yeh, R.-F., Wythe, J. D., Ivey, K. N., Bruneau, B. G., Stainier, D. Y. R. and Srivastava, D. (2008). miR-126 regulates angiogenic signaling and vascular integrity. *Dev. Cell* **15**, 272–284.
- Friedman, Y., Balaga, O. and Linial, M. (2013). Working together: combinatorial regulation by microRNAs. *Adv. Exp. Med. Biol.* **774**, 317–337.

- Goldie, B. J., Dun, M. D., Lin, M., Smith, N. D., Verrills, N. M., Dayas, C. V. and Cairns, M. J.** (2014). Activity-associated miRNA are packaged in Map1b-enriched exosomes released from depolarized neurons. *Nucleic Acids Res.* **42**, 9195-9208.
- Gregory, P. A., Bert, A. G., Paterson, E. L., Barry, S. C., Tsykin, A., Farshid, G., Vadas, M. A., Khew-Goodall, Y. and Goodall, G. J.** (2008). The miR-200 family and miR-205 regulate epithelial to mesenchymal transition by targeting ZEB1 and SIP1. *Nat. Cell Biol.* **10**, 593-601.
- Guss, K. A. and Ettensohn, C. A.** (1997). Skeletal morphogenesis in the sea urchin embryo: Regulation of primary mesenchyme gene expression and skeletal rod growth by ectoderm-derived cues. *Development* **124**, 1899-1908.
- Gustafson, E. A. and Wessel, G. M.** (2010). Exogenous RNA is selectively retained in the small micromeres during sea urchin embryogenesis. *Mol. Reprod. Dev.* **77**, 836.
- Hart, M. W. and Strathmann, R. R.** (1994). Functional consequences of phenotypic plasticity in echinoid larvae. *Biol. Bull.* **186**, 291-299.
- Huang, S. and He, X.** (2010). microRNAs: tiny RNA molecules, huge driving forces to move the cell. *Protein Cell* **1**, 916-926.
- Inui, M., Martello, G. and Piccolo, S.** (2010). MicroRNA control of signal transduction. *Nat. Rev. Mol. Cell Biol.* **11**, 264-275.
- Iwama, H., Masaki, T. and Kuriyama, S.** (2007). Abundance of microRNA target motifs in the 3'-UTRs of 20527 human genes. *FEBS Lett.* **581**, 1805-1810.
- Khaner, O. and Wilt, F.** (1991). Interactions of different vegetal cells with mesomeres during early stages of sea urchin development. *Development* **112**, 881-890.
- Kim, H. H., Kim, P., Phay, M. and Yoo, S.** (2015). Identification of precursor microRNAs within distal axons of sensory neuron. *J. Neurochem.* **134**, 193-199.
- Knapp, R. T., Wu, C.-H., Mobilia, K. C. and Joester, D.** (2012). Recombinant sea urchin vascular endothelial growth factor directs single-crystal growth and branching in vitro. *J. Am. Chem. Soc.* **134**, 17908-17911.
- Koga, H., Matsubara, M., Fujitani, H., Miyamoto, N., Komatsu, M., Kiyomoto, M., Akasaka, K. and Wada, H.** (2010). Functional evolution of Ets in echinoderms with focus on the evolution of echinoderm larval skeletons. *Dev. Genes Evol.* **220**, 107-115.
- Körner, C., Keklikoglou, I., Bender, C., Wörner, A., Münnstermann, E. and Wiemann, S.** (2013). MicroRNA-31 sensitizes human breast cells to apoptosis by direct targeting of protein kinase C epsilon (PKC $\epsilon$ ). *J. Biol. Chem.* **288**, 8750-8761.
- Kuhnert, F., Mancuso, M. R., Hampton, J., Stankunas, K., Asano, T., Chen, C.-Z. and Kuo, C. J.** (2008). Attribution of vascular phenotypes of the murine Egfl locus to the microRNA miR-126. *Development* **135**, 3989-3993.
- Kye, M.-J., Liu, T., Levy, S. F., Xu, N. L., Groves, B. B., Bonneau, R., Lao, K. and Kosik, K. S.** (2007). Somatodendritic microRNAs identified by laser capture and multiplex RT-PCR. *RNA* **13**, 1224-1234.
- Lapraz, F., Röttinger, E., Duboc, V., Range, R., Duloquin, L., Walton, K., Wu, S.-Y., Bradham, C., Loza, M. A., Hibino, T. et al.** (2006). RTK and TGF-beta signaling pathways genes in the sea urchin genome. *Dev. Biol.* **300**, 132-152.
- Lewis, B. P., Burge, C. B. and Bartel, D. P.** (2005). Conserved seed pairing, often flanked by adenines, indicates that thousands of human genes are microRNA targets. *Cell* **120**, 15-20.
- Li, Y. and Kowdley, K.** (2012). MicroRNAs in common human diseases. *Genomics Proteomics Bioinformatics* **10**, 246-253.
- Lim, L. P., Lau, N. C., Garrett-Engle, P., Grimson, A., Schelter, J. M., Castle, J., Bartel, D. P., Linsley, P. S. and Johnson, J. M.** (2005). Microarray analysis shows that some microRNAs downregulate large numbers of target mRNAs. *Nature* **433**, 769-773.
- Lyons, D. C., Martik, M. L., Saunders, L. R. and McClay, D. R.** (2014). Specification to biomineralization: following a single cell type as it constructs a skeleton. *Integr. Comp. Biol.* **54**, 723-733.
- Martello, G., Zucchini, L., Inui, M., Montagner, M., Adorno, M., Mamidi, A., Morsut, L., Soligo, S., Tran, U., Dupont, S. et al.** (2007). MicroRNA control of Nodal signalling. *Nature* **449**, 183-188.
- McClay, D. R., Cannon, G. W., Wessel, G. M., Fink, R. D. and Marchase, R. B.** (1983). Patterns of antigenic expression in early sea urchin development. In *Time, Space, and Pattern in Embryonic Development* (ed. W. R. Jeffrey and R. A. Raff), pp. 157-169. New York: A. R. Liss.
- McGonnell, I. M., Graham, A., Richardson, J., Fish, J. L., Depew, M. J., Dee, C. T., Holland, P. W. H. and Takahashi, T.** (2011). Evolution of the Alx homeobox gene family: parallel retention and independent loss of the vertebrate Alx3 gene. *Evol. Dev.* **13**, 343-351.
- McIntyre, D. C., Seay, N. W., Croce, J. C. and McClay, D. R.** (2013). Short-range Wnt5 signaling initiates specification of sea urchin posterior ectoderm. *Development* **140**, 4881-4889.
- Meng, F., Henson, R., Wehbe-Janek, H., Ghoshal, K., Jacob, S. T. and Patel, T.** (2007). MicroRNA-21 regulates expression of the PTEN tumor suppressor gene in human hepatocellular cancer. *Gastroenterology* **133**, 647-658.
- Minokawa, T., Rast, J. P., Arenas-Mena, C., Franco, C. B. and Davidson, E. H.** (2004). Expression patterns of four different regulatory genes that function during sea urchin development. *Gene Expr. Patterns* **4**, 449-456.
- Naguibneva, I., Ameyar-Zazoua, M., Nonne, N., Polesskaya, A., Ait-Si-Ali, S., Groisman, R., Souidi, M., Pritchard, L. L. and Harel-Bellan, A.** (2006). An LNA-based loss-of-function assay for micro-RNAs. *Biomed. Pharmacother.* **60**, 633-638.
- Nicolas, F. E.** (2011). Experimental validation of microRNA targets using a luciferase reporter system. *Methods Mol. Biol.* **732**, 139-152.
- Niehrs, C.** (2004). Regionally specific induction by the Spemann-Mangold organizer. *Nat. Rev. Genet.* **5**, 425-434.
- Oliveri, P., Davidson, E. H. and McClay, D. R.** (2003). Activation of pmar1 controls specification of micromeres in the sea urchin embryo. *Dev. Biol.* **258**, 32-43.
- Pedioli, D. M. L., Karpanen, T., Dabouras, V., Jurisic, G., van de Hoek, G., Shin, J. W., Marino, D., Kalin, R. E., Leidel, S., Cinelli, P. et al.** (2010). miR-31 functions as a negative regulator of lymphatic vascular lineage-specific differentiation in vitro and vascular development in vivo. *Mol. Cell. Biol.* **30**, 3620-3634.
- Pennington, J. T. and Strathmann, R. R.** (1990). Consequences of the calcite skeletons of planktonic echinoderm larvae for orientation, swimming, and shape. *Biol. Bull.* **179**, 121-133.
- Rafiq, K., Cheers, M. S. and Ettensohn, C. A.** (2012). The genomic regulatory control of skeletal morphogenesis in the sea urchin. *Development* **139**, 579-590.
- Revilla-i-Domingo, R., Oliver, P. and Davidson, E. H.** (2007). A missing link in the sea urchin embryo gene regulatory network: hesC and the double-negative specification of micromeres. *Proc. Natl. Acad. Sci. USA* **104**, 12383-12388.
- Rottinger, E., Saudemont, A., Duboc, V., Besnard, L., McClay, D. and Lepage, T.** (2008). FGF signals guide migration of mesenchymal cells, control skeletal morphogenesis and regulate gastrulation during sea urchin development. *Development* **135**, 353-365.
- Rozen, S. and Skaltsky, H.** (2000). Primer3 on the WWW for general users and for biologist programmers. *Methods Mol. Biol.* **132**, 365-386.
- Saudemont, A., Haillot, E., Mekpoh, F., Bessodes, N., Quirin, M., Lapraz, F., Duboc, V., Röttinger, E., Range, R., Oisel, A. et al.** (2010). Ancestral regulatory circuits governing ectoderm patterning downstream of Nodal and BMP2/4 revealed by gene regulatory network analysis in an echinoderm. *PLoS Genet.* **6**, e1001259.
- Saunders, L. R. and McClay, D. R.** (2014). Sub-circuits of a gene regulatory network control a developmental epithelial-mesenchymal transition. *Development* **141**, 1503-1513.
- Schmittgen, T. D.** (2010). miR-31: a master regulator of metastasis? *Future Oncol.* **6**, 17-20.
- Schuldt, A.** (2005). MicroRNAs diversify in Drosophila development. *Nat. Cell Biol.* **7**, 781.
- Selbach, M., Schwanhäusser, B., Thierfelder, N., Fang, Z., Khanin, R. and Rajewsky, N.** (2008). Widespread changes in protein synthesis induced by microRNAs. *Nature* **455**, 58-63.
- Sethi, A. J., Angerer, R. C. and Angerer, L. M.** (2014). Multicolor labeling in developmental gene regulatory network analysis. *Methods Mol. Biol.* **1128**, 249-262.
- Sharma, T. and Ettensohn, C. A.** (2010). Activation of the skeletogenic gene regulatory network in the early sea urchin embryo. *Development* **137**, 1149-1157.
- Sharma, T. and Ettensohn, C. A.** (2011). Regulative deployment of the skeletogenic gene regulatory network during sea urchin development. *Development* **138**, 2581-2590.
- Slusarski, D. C., Corces, V. G. and Moon, R. T.** (1997). Interaction of Wnt and a Frizzled homologue triggers G-protein-linked phosphatidylinositol signalling. *Nature* **390**, 410-413.
- Sodergren, E., Weinstock, G. M., Davidson, E. H., Cameron, R. A., Gibbs, R. A., Angerer, R. C., Angerer, L. M., Arnone, M. I., Burgess, D. R., Burke, R. D. et al.** (2006). The genome of the sea urchin Strongylocentrotus purpuratus. *Science* **314**, 941-952.
- Song, J. L., Stoeckius, M., Maaskola, J., Friedländer, M., Stepicheva, N., Juliano, C., Lebedeva, S., Thompson, W., Rajewsky, N. and Wessel, G. M.** (2012). Select microRNAs are essential for early development in the sea urchin. *Dev. Biol.* **362**, 104-113.
- Staton, A. A. and Giraldez, A. J.** (2011). Use of target protector morpholinos to analyze the physiological roles of specific miRNA-mRNA pairs in vivo. *Nat. Protoc.* **6**, 2035-2049.
- Stepicheva, N. and Song, J.** (2014). High throughput microinjections of sea urchin zygotes. *J. Vis. Exp.*, e50841.
- Stepicheva, N., Nigam, P. A., Siddam, A. D., Peng, C. F. and Song, J. L.** (2015). microRNAs regulate  $\beta$ -catenin of the Wnt signalling pathway in early sea urchin development. *Dev. Biol.* **402**, 127-141.
- Stuelten, C. H. and Salomon, D.** (2010). miR-31 in cancer: location matters. *Cell Cycle* **9**, 4608.
- Sun, Z. and Ettensohn, C. A.** (2014). Signal-dependent regulation of the sea urchin skeletogenic gene regulatory network. *Gene Expr. Patterns* **16**, 93-103.
- Thum, T., Gross, C., Fiedler, J., Fischer, T., Kissler, S., Bussen, M., Galuppo, P., Just, S., Rottbauer, W., Frantz, S. et al.** (2008). MicroRNA-21 contributes to myocardial disease by stimulating MAP kinase signalling in fibroblasts. *Nature* **456**, 980-984.

- Uz, E., Alanay, Y., Aktas, D., Vargel, I., Gucer, S., Tuncbilek, G., von Eggeling, F., Yilmaz, E., Deren, O., Posorski, N. et al.** (2010). Disruption of ALX1 causes extreme microphthalmia and severe facial clefting: expanding the spectrum of autosomal-recessive ALX-related frontonasal dysplasia. *Am. J. Hum. Genet.* **86**, 789-796.
- Valastyan, S. and Weinberg, R. A.** (2010). miR-31: a crucial overseer of tumor metastasis and other emerging roles. *Cell Cycle* **9**, 2124-2129.
- Vidavsky, N., Addadi, S., Mahamid, J., Shimoni, E., Ben-Ezra, D., Shpigel, M., Weiner, S. and Addadi, L.** (2014). Initial stages of calcium uptake and mineral deposition in sea urchin embryos. *Proc. Natl. Acad. Sci. USA* **111**, 39-44.
- Wang, L., Fu, C., Fan, H., Du, T., Dong, M., Chen, Y., Jin, Y., Zhou, Y., Deng, M., Gu, A. et al.** (2013). miR-34b regulates multiciliogenesis during organ formation in zebrafish. *Development* **140**, 2755-2764.
- Wienholds, E., Kloosterman, W. P., Miska, E., Alvarez-Saavedra, E., Berezikov, E., de Bruijn, E., Horvitz, H. R., Kauppinen, S. and Plasterk, R. H. A.** (2005). MicroRNA expression in zebrafish embryonic development. *Science* **309**, 310-311.
- Wilczynska, A. and Bushell, M.** (2015). The complexity of miRNA-mediated repression. *Cell Death Differ.* **22**, 22-33.
- Wilt, F. H.** (1999). Matrix and mineral in the sea urchin larval skeleton. *J. Struct. Biol.* **126**, 216-226.
- Wilt, F. H.** (2002). Biominerization of the spicules of sea urchin embryos. *Zoolog. Sci.* **19**, 253-261.
- Wu, S.-Y. and McClay, D. R.** (2007). The Snail repressor is required for PMC ingressions in the sea urchin embryo. *Development* **134**, 1061-1070.
- Xu, R. S., Wu, X. D., Zhang, S. Q., Li, C. F., Yang, L., Li, D. D., Zhang, B. G., Zhang, Y., Jin, J. P. and Zhang, B.** (2013). The tumor suppressor gene RhoBTB1 is a novel target of miR-31 in human colon cancer. *Int. J. Oncol.* **42**, 676-682.
- Yaguchi, S., Yaguchi, J., Angerer, R. C., Angerer, L. M. and Burke, R. D.** (2010). TGF $\beta$  signaling positions the ciliary band and patterns neurons in the sea urchin embryo. *Dev. Biol.* **347**, 71-81.
- Yamagishi, M., Nakano, K., Miyake, A., Yamochi, T., Kagami, Y., Tsutsumi, A., Matsuda, Y., Sato-Otsubo, A., Muto, S., Utsunomiya, A. et al.** (2012). Polycomb-mediated loss of miR-31 activates NIK-dependent NF- $\kappa$ B pathway in adult T cell leukemia and other cancers. *Cancer Cell* **21**, 121-135.
- Yuan, H., Kajiyama, H., Ito, S., Yoshikawa, N., Hyodo, T., Asano, E., Hasegawa, H., Maeda, M., Shibata, K., Hamaguchi, M. et al.** (2013). ALX1 induces snail expression to promote epithelial-to-mesenchymal transition and invasion of ovarian cancer cells. *Cancer Res.* **73**, 1581-1590.